Journal of Power Sources 196 (2011) 5357–5363

Contents lists available at ScienceDirect

Journal of Power Sources

journal homepage: www.elsevier.com/locate/jpowsour

# State-of-health monitoring of lithium-ion batteries in electric vehicles by on-board internal resistance estimation

Jürgen Remmlinger[a,*], Michael Buchholz[a], Markus Meiler[b], Peter Bernreuter[b], Klaus Dietmayer[a]

[a] Institute of Measurement, Control, and Microtechnology, Ulm university, Albert-Einstein-Allee 41, D-89081 Ulm, Germany
[b] Deutsche ACCUmotive GmbH & Co. KG, Neue Straße 95, D-73230 Kirchheim/Teck, Germany

ARTICLE INFO

*Article history:*
Received 11 June 2010
Received in revised form 23 July 2010
Accepted 5 August 2010
Available online 20 August 2010

*Keywords:*
Lithium-ion battery
State-of-health
On-board diagnosis
Internal resistance

ABSTRACT

For reliable and safe operation of lithium-ion batteries in electric or hybrid vehicles, diagnosis of the cell degradation is necessary. This can be achieved by monitoring the increase of the internal resistance of the battery cells over the whole lifetime of the battery. In this paper, a method to identify the internal resistance in a hybrid vehicle is presented. Therefore, a special purpose model deduced from an equivalent circuit is developed. This model contains parameters depending on the degradation of the battery cell. To achieve the required robustness and stable results under these conditions, the method uses specific signal intervals occurring during normal operation of the battery in a hybrid vehicle. This identification signal has a defined timespan and occurs regularly. The identification is done on vehicle measurement data of terminal cell voltage and current collected with a usual vehicle sampling rate. Using the adapted internal resistance value in the model, a degradation index is calculated by compensating other influences, e.g. battery temperature. This task is the main challenge, as the impact of the temperature on the resistance, for example, is one order of magnitude higher than the influence of the degradation for the investigated lithium-ion cell. The developed estimation and monitoring method is validated with measurement data from single cells and shows good results and very low computational effort.



## 1. Introduction

A task that has to be solved for the application of batteries in vehicles with an electric drive train is the determination of the actual state-of-health (SOH) of the battery cells. The knowledge of the SOH can be used to recognize an ongoing or abrupt degradation of the battery cells and to prevent a possible failure of the electric system and, accordingly, the vehicle. As the internal resistance of a battery cell is one of the main characteristics that are affected by degradation, the determination of the SOH can be done by monitoring the internal resistance of the battery cell during operation of the battery. Additionally, the internal resistance of the battery cells can be used for other purposes, e.g. a short or midterm power prediction.

Methods for determining the degradation of battery cells usually use impedance spectroscopy and are carried out under laboratory conditions [1,2]. As these methods are usually model based, there are multiple battery models of varying complexity for different purposes [3,4]. For a vehicle application, these methods are not applicable because no laboratory testing equipment is available.

Existing methods developed for the use within a vehicle use filter technologies to determine the conditions of the battery cells. In these approaches, the internal resistance is a parameter assumed to be known. An exception is [5,6], where the states and parameters are estimated using a dual filter concept. This concept is computational expensive and can only be implemented on a very powerful vehicle electronic control unit (ECU). For this reason, methods requiring only a standard ECU have to be developed.

In this contribution, the internal resistance of a battery cell is identified on-board periodically with a minimum of processing power and memory capacity. Therefore, a special purpose model deduced from an equivalent circuit is used. This model contains parameters depending on the degradation of the battery cell. To achieve the required robustness and stable results under these conditions, the method uses specific signal intervals occurring during normal operation of the battery in a hybrid vehicle. This identification signal has a defined timespan and occurs regularly.

To determine the progress of the degradation, various other influences on the internal resistance besides the degradation of the battery cell have to be considered. In this contribution, this task is solved for the investigated lithium-ion cells implicitly by the chosen identification signals, where the battery conditions can be assumed to be homogeneous over all cells and the temperature is therefore measurable by the external temperature sensors. The developed estimation and monitoring method is validated with

* Corresponding author. Tel.: +49 731 50 26308; fax: +49 731 50 26301.
*E-mail address:* juergen.remmlinger@uni-ulm.de (J. Remmlinger).

0378-7753/$ – see front matter © 2010 Elsevier B.V. All rights reserved.
doi:10.1016/j.jpowsour.2010.08.035

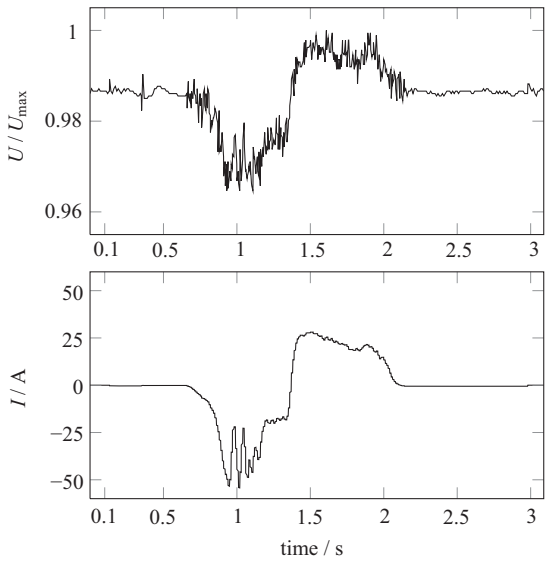


**Fig. 1.** Identification signal at start of combustion engine at $\theta = 30\,^{\circ}C$.

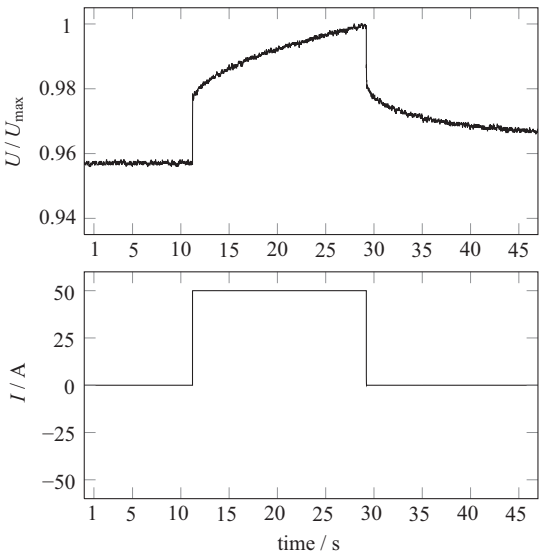


**Fig. 2.** Reference signal: current pulse at $\theta = 30\,^{\circ}C$.

measurement data from single cells and shows good results and very low computational effort.

The underlying experiments are presented in Section 2 and the derived model for the method in Section 3. The developed monitoring method itself is described in Section 4. The contribution concludes with a summary in Section 5.

## 2. Design of experiment

The presented method is designed for a vehicle on-board application. Therefore, recorded data from inner-city driving of a hybrid vehicle were analyzed and promising sequences for a determination of a degradation index were selected. These sequences had to be tested for their ability to indicate the degradation. Thus, the sequences were transferred to a laboratory battery testing system by setting the measured current as current demand for the testing. If cells in a vehicle battery are connected in series, this methodology has the advantage that the current demand does not have to be scaled at varying cell numbers. The tests were done in a climate chamber at temperatures of $-20\,^{\circ}C$, $-8\,^{\circ}C$, $12\,^{\circ}C$, $30\,^{\circ}C$, and $50\,^{\circ}C$.

A promising timespan for the on-board determination of the internal resistance is the start of the combustion engine of the hybrid vehicle. The current and terminal voltage measured in the vehicle for this period are plotted in Fig. 1. The signal has an overall duration of 2.5 s and is a strong excitation of the battery. Therefore, the signal is expected to be a good identification signal. Further advantages of this signal are its short duration, which guarantees a low identification effort, its unchanging shape, which allows an identification with always the same current magnitude, and its regular occurrence in the driving profile. It also appears at the beginning of the operation after longer resting periods and allows an identification of the internal resistance of the balanced battery cell. Therefore, the signal was included in the testing profile several times.

To determine a reference value of the internal resistance, current pulse signals have been inserted into the testing cycle regularly. One of these current pulses and the measured terminal voltage are shown in Fig. 2. As this pulse is a strong excitation of the battery cell, it is a reliable reference signal. Resting times with a current demand of zero were included in the testing cycle before and after these current pulses, but also between the vehicle driving cycle, to allow dynamic effects to decay.

To compare the results of the presented method, the tests were carried out on a new and a degraded typical 6.5 Ah high-power lithium-ion battery cell used in hybrid vehicle batteries. The electrical behaviour of these cells is described in [7,8]. The degradation was done by thermal aging, i.e. the cell was stored at temperatures over $50\,^{\circ}C$ to accelerate the degradation. This thermal aging can be seen as approximation to a usual calendaric aging in a vehicle [9]. After this thermal aging process, the battery cell was subject to intensive testing. Thereby, the complex internal resistance and the capacity were determined.

## 3. Battery modeling

### 3.1. Main effects represented in a battery model

A general battery model to describe the electrical behavior is usually derived from an equivalent circuit (EC) as shown in Fig. 3. The main parts of this EC are an ideal voltage source, an ohmic resistance and two parallel connections of an ohmic resistor with a capacitor. The ideal voltage source is representing the open-circuit voltage and the ohmic resistance the resistance of the materials. The parallel connections of an ohmic resistor and a capacitor describe the time-dependent overvoltage occurring at the battery cell terminal while the battery is charged or discharged. These parallel connections stand for the effects caused by polarization and diffusion. The parametrization values of the resistors and capacitors are depending on the particular operating point of the battery and the cell degradation. Therefore, they are time-variant and change with temperature, state-of-charge (SOC), power demand, and degradation.

To easily analyze the networks created from resistances and capacitors, corresponding differential equations are transformed

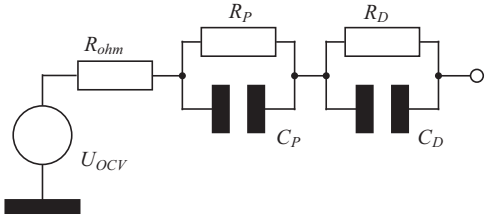


**Fig. 3.** Equivalent circuit of battery cell.

**Table 1**
Typical ranges for the parameters of the EC for one cell due to operation conditions.

| | Ohmic resistance | Polarization | Diffusion |
|---|---|---|---|
| Gain | $R_{ohm}$ | 0.2...2.5 $R_{ohm}$ | 0.5...4 $R_{ohm}$ |
| Time constant | – | 0.01...3 s | 4...30 s |

into the Laplace domain. For example, a *RC*-parallel connection specifies a first-order low-pass transfer-function ($PT_1$). The parameters *R* and *C* of the parallel connection can be converted to gain and time constant of the $PT_1$ element. The linear equations in the Laplace domain describe the battery behavior only in one operation point for fixed parameters. The typical parameter variations of the investigated lithium-ion battery cells within the operating range are shown in Table 1.

Due to the large variation of the values, the determination of the degradation dependent part of the change in the internal resistance is a challenging task. As the degradation has a main influence on the activity of the electrolyte, the values of the polarization and diffusion effect are affected by the degradation, which is observable in enlarged gains and time constants of the $PT_1$ elements.

Furthermore, the term "internal resistance" is not clear defined. In general linguistic usage, internal resistance usually means the ohmic resistance of the EC, which corresponds with the intersection of an impedance spectrum of the battery cell with the real axis. Depending on the EC referred to, other definitions are also possible. As explained in the following section, a separate identification of all parts of the EC is neither possible nor necessary for the described method in an on-board application. The internal resistance used in this contribution is approximately a sum of the ohmic resistance and the gain of the $PT_1$ element representing the polarization effect. This internal resistance is degradation dependent.

Temperature, state-of-charge, and current magnitude also affect the internal resistance of lithium-ion cells. The significance of these influences vary strongly with the battery chemistry. The investigations in this contribution are based on typical 6.5 Ah high-power lithium-ion cells for hybride vehicle applications [7]. In the operation region of a hybrid vehicle, there has been found a negligible dependence of the internal resistance on the state-of-charge as long as no mass transport limitations (i.e. diffusion effects) are involved [7,8]. Like in many other approaches, e.g. [6,10,11], the dependence of the internal resistance on the current magnitude is also neglected. However, the method uses always the same identification signal at start of the combustion engine, which leads to comparable values of the model parameters at least for degradation monitoring. Nevertheless, it is necessary to compensate the influence of the varying temperature of the battery, as this has immense effect on the values of the internal resistance. The solution to this task is further described in Section 4.3.

With the described general battery model according to Fig. 3, the reference pulse signals were evaluated. The internal resistance values, i.e. the sum of the ohmic resistance and the gain of the polarization element, identified at the different temperatures for the new and the degraded cell are shown in Fig. 4. It is obvious that there exists a strong temperature dependence of the internal resistance, but also a much weaker dependence on the degradation of the battery cell. From electrochemical impedance spectroscopy after the aging, the internal resistance was found to be approximately 20% higher than the one of the new cell which corresponds with the shown results. Due to the temperature dependence, the internal resistance enlarges from high to low temperatures with a factor of 40 and is much more sensitiv to the temperature changes than to degradation. Therefore, a determination of the degradation from the internal resistance is only possible if an accurate temperature measurement is available. These resistance values, according to the definition of the internal resistance used in this contribution, are extracted parameter values of an EC as shown in Fig. 3. Although it is possible to identify all parameters of this EC with the reference signal, only the sum of the ohmic resistance and the gain of the polarization element is plotted so that it can be compared with the estimated values in the on-board application. This has the additional advantage that these resistance values can be compared even if the reference signal and the signal in the application have a different duration as this is the case here.

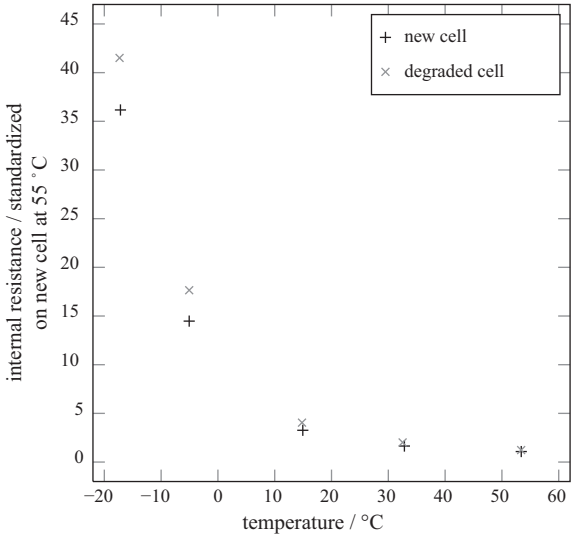


**Fig. 4.** Identified internal resistance values at several temperatures with reference current pulse excitation.

### 3.2. Adapted model for an on-board application

For identification of the elements of the general battery cell model as shown before, the identification signal has to have special attributes, e.g. an excitation in a wide frequency range. In an on-board application using only the common signals occurring during operation, these attributes are not always available. Therefore, an adapted model for this application is derived.

The identification signal "starting of the combustion engine" shows a strong excitation of the battery cell but has a short overall duration as shown in Section 2. As the general battery model exists of two $PT_1$ elements with very different time constants and one time constant much larger than the duration of the excitation signal, they cannot both be identified with this identification signal [12].

The behavior of such a stiff system is demonstrated in Fig. 5. The two linear systems are set up as

$$G_1(s) = \frac{1}{1 + T_1 s} \tag{1}$$

$$G_2(s) = \frac{1}{(1 + T_1 s)} + \frac{1}{(1 + T_2 s)} \tag{2}$$

with the Laplace variable *s* and $T_2 = 400\,T_1$, which is a usual ratio for time constants in battery dynamics. The systems are excited with a composition of different signals:

$$u(t) = \begin{cases} 0 & \text{for } 0 \le t < 1 \\ -\sin(2\pi t) & \text{for } 1 \le t < 2 \\ 0 & \text{for } 2 \le t < 4 \\ 1 & \text{for } t \ge 4 \end{cases}. \tag{3}$$

Both system outputs equal each other for the sine wave input but differ in the step response. As the identification signal in the application is similar to the sine wave, it is obvious that not the whole general model can be determined. Again, that identification

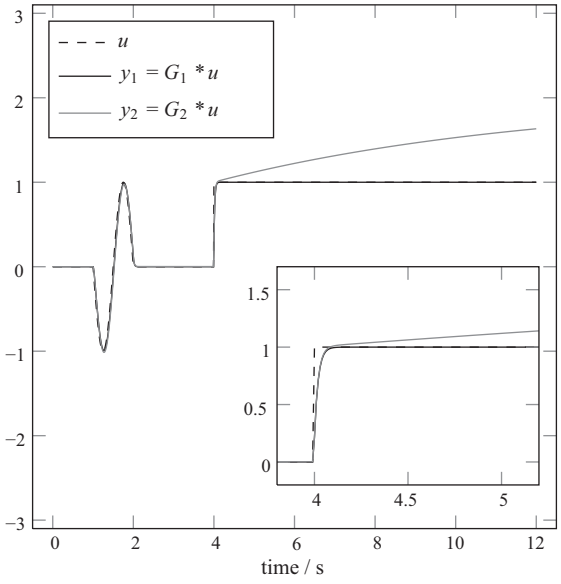


**Fig. 5.** Comparison of a stiff system ($T_2 = 400\ T_1$) with an akin system ($T_1$).

effort is not necessary to be done here because the internal resistance used in this contribution is a sum of the ohmic resistance an the gain of the polarization effect. Instead, a simplified model is used neglecting the diffusion effects. Furthermore, the ohmic resistance is integrated into the remaining $PT_1$ element. This is possible because the time constant is not considerably larger than the sampling time of the measurement data. Although not being a general description of the degraded cell, this simplified model is suitable for an on-board monitoring method with dynamic excitation, since its parameters are still degradation dependent.

The simplified model has to be expressed in a digital realization for model identification and the computation on the vehicle ECU. For this reason, the model is transferred from the continuous-time frequency domain (Laplace domain) to the discrete-time frequency domain ($z$-domain). In the $z$-domain, the model behavior can be analyzed at a defined sampling time. For the purpose of model identification, the $z$-domain equation can be transformed in a discrete-time difference equation that is linear in its parameters. These parameters can be estimated with a least-squares algorithm.

The resulting $z$-domain equation for the simplified battery model is

$$G(z) = \frac{U(z) - U_{OCV}}{I(z)} = \frac{b_1 z^{-1}}{1 + a_1 z^{-1}}. \tag{4}$$

This equation equals the time-discrete difference equation

$$u_{d,k} = -a_1 u_{d,k-1} + b_1 i_{k-1} \tag{5}$$

with the sample marker $k$ and $u_d = u - u_{OCV}$. That means the two parameters $a_1$ and $b_1$ must be estimated from the time-series signal of terminal voltage after subtraction of the actual open-circuit voltage (OCV) and the current. This can be done by a linear parameter estimation method as the parameters appear in a linear form in the equation. From those parameters, the internal resistance can be calculated by

$$R_i(\vartheta) = \frac{b_1(\vartheta)}{1 + a_1(\vartheta)}, \tag{6}$$

being dependent on the battery cell temperature $\vartheta$.

The explained identification method for the internal resistance offers all possibilities to be implemented in an on-board identification system. This implementation and the calculation of the degradation index are explained in the following section.

## 4. On-board monitoring algorithm

### 4.1. Demands on an on-board monitoring algorithm

A method monitoring the resistance has to meet specific requirements for being applicable in vehicles. This was taken into account in the development of this method. As neither special testing hardware nor expensive sensors are available in the vehicle environment, the method works with regular recorded signals which are necessary for a safe operation of the battery system anyway. The measurements in vehicles are done with a relatively high sampling time and are affected by the reduced accuracy of the sensors. Therefore, the implemented algorithm has to be adapted for this high sampling time which is done through model adaptions as explained before.

For the computational methods, limiting factors are the processing power and the memory capacity of the electronic control unit (ECU). On the one hand, the applicability of the method is guaranteed by the special point in time used for the measurement of the identification signal and through the adapted model. The limited amount of data points used for the identification ensures little identification effort as well as the adapted battery cell model containing only few parameters. But on the other hand, it also depends on the used techniques for solving every single task of the monitoring algorithm as explained in the following.

### 4.2. On-board determination of the internal resistance

The identification of the internal resistance is done with the special identification signals of terminal voltage and current at the start of the combustion engine of the hybrid vehicle with the adapted model described in Section 3.2. The parameters of this linear model can be identified using a linear least-squares identification algorithm [13].

The identification problem is of the form

$$y_k = \boldsymbol{m}_k^{\mathrm{T}} \boldsymbol{\Theta} + e_k \quad \text{with} \quad (k = n+1, \ldots, n+N). \tag{7}$$

In this case, the model output $y_k$ is the time-series signal of the terminal voltage after subtraction of the OCV, $\boldsymbol{m}_k$ consist of the delayed output signal and of the input signal current of the cell, the parameter vector $\boldsymbol{\Theta}$ is formed as $[a_1\ b_1]^{\mathrm{T}}$, and $e_k$ is a potentially occurring additional disturbance, e.g. measurement noise. This identification can be performed in one single step, but in this case larger arrays have to be handled and a matrix inversion must be calculated. Therefore, a regressive formulation of the linear least-squares algorithm is used [13]:

$$\boldsymbol{P}_k = \boldsymbol{P}_{k-1} - \boldsymbol{P}_{k-1}\boldsymbol{m}_k[1 + \boldsymbol{m}_k^{\mathrm{T}}\boldsymbol{P}_{k-1}\boldsymbol{m}_k]^{-1}\boldsymbol{m}_k^{\mathrm{T}}\boldsymbol{P}_{k-1} \tag{8}$$

$$\boldsymbol{k}_k = \boldsymbol{P}_{k-1}\boldsymbol{m}_k[1 + \boldsymbol{m}_k^{\mathrm{T}}\boldsymbol{P}_{k-1}\boldsymbol{m}_k]^{-1} \tag{9}$$

$$\boldsymbol{\Theta}_k = \boldsymbol{\Theta}_{k-1} + \boldsymbol{k}_k[y_k - \boldsymbol{m}_k^{\mathrm{T}}\boldsymbol{\Theta}_{k-1}]. \tag{10}$$

The algorithm starts with predefined values for the parameter vector $\boldsymbol{\Theta}_0$ and the covariance matrix $\boldsymbol{P}_0$ at $k = 1$. Afterwards, new values for $\boldsymbol{\Theta}_k$ and $\boldsymbol{P}_k$ are calculated iteratively for the complete data set using the correction term $\boldsymbol{k}_k$ up to $k = N$, with $N$ the number of data points. $\boldsymbol{\Theta}_0$ can be set to zeros or near to the expected identification value. There has not been found a dependency of the identification result on the starting parameters as long as $\boldsymbol{P}_0$ is selected large enough to allow a variation of the parameter vector.

The internal resistance can be calculated from the parameter vector using Eq. (6). Furthermore, the model can be used for other purposes as short-time power predictions. For this application, the model adaptions to the identification signal have to be regarded. A

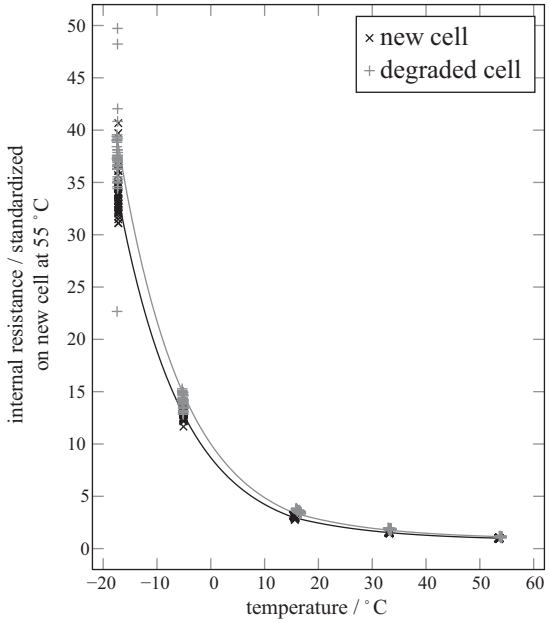


**Fig. 6.** Identified internal resistance values at several temperatures with excitation start of combustion engine.

power prediction is only possible in scenarios in which the operation signal has similar dynamics as the excitation signal used for model identification due to the neglected diffusion effect.

The results for the recursive identification are shown in Fig. 6. The values for the internal resistance are plotted against temperature for a new and an degraded cell. The values for the cells show a large temperature dependence but also a degradation dependence. The overall characteristic of the identified resistance-temperature behavior is comparable to those found with the complete model for the sum of ohmic and polarization resistance shown in Fig. 4. There can also be found only a small variation of the identified internal resistance values at one temperature except for the values at −20 °C, suggesting a good robustness of the method. The larger variance at −20 °C presumably occurs because of the varying, not constant inner battery temperature influenced by the internal heat produced on-load due to the internal resistance.

### 4.3. Temperature compensation and calculation of a degradation index

To express the degradation in a numerical value, a degradation index $k_d$ is calculated. It specifies the degradation state of a battery cell with respect to its internal resistance independent of the actual cell temperature of the measurement. For a new cell, the degradation index is 1 and increases with the internal resistance during operation.

For the calculation of the resistance dependent degradation index, the temperature dependency of the determined internal resistance values has to be eliminated. Therefore, a characteristic curve

$$R_{i,new}(\theta) = a\, e^{-b\theta} + c \tag{11}$$

with positive parameters $a$, $b$ and $c$ is fitted to the resistance values $R_{i,new}$ and the corresponding temperatures $\theta$ of the new cell to retain an reference curve for the temperature dependency of the internal resistance. The form of Eq. (11) is chosen because of the temperature dependence following an Arrhenius law [14] and the curve accurately meets the data points. The curve is plotted in Fig. 6 for the new cell (black line).

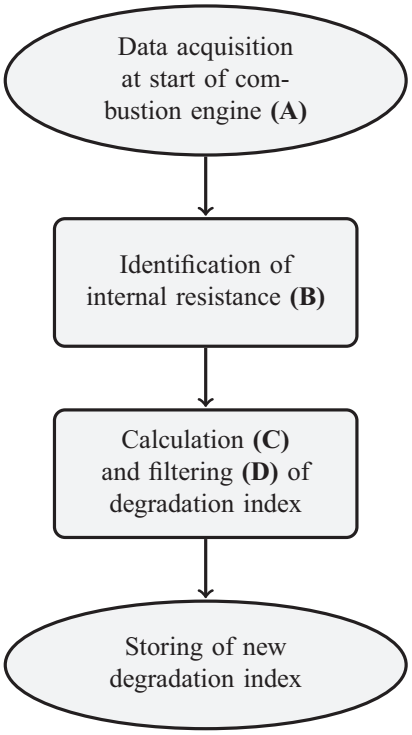


**Fig. 7.** Operation chart of monitoring algorithm.

The calculation of the degradation index $k_d$ is now performed by solving the equation

$$R_{i,act} = k_d R_{i,new}(\theta_{act}) \tag{12}$$

for $k_d$ with the actual values $R_{i,act}$ and $\theta_{act}$. In other words, the scaling factor between the theoretical resistance value of the new cell at the actual temperature and the actual internal resistance is calculated as degradation index. The actual cell temperature $\theta_{act}$ can be assumed to be known if only resistance estimates after long resting periods are used. Then, the cells are balanced and have the same temperature as the ambience, which can be measured accurately enough. For an on-board realization, the characteristic curve of the new cell is stored in a look-up table with an appropriate amount of nodes to retain all intermediate values through linear interpolation. The degradation index $k_d$ for the degraded cell was determined to 1.18 and equals almost the increase of the internal resistance of 20%. The scaled curve for this degraded cell is also plotted in Fig. 6 (gray line).

To calculate the degradation index, it is necessary to know the characteristic curve of the internal resistance over temperature for the new cell. It can either be obtained by measuring the characteristic for every cell before the first operation in a laboratory, or by using one defined characteristic for all cells if they do not differ significantly from this reference.

### 4.4. Overall scheduling of the monitoring algorithm

The monitoring method is summarized in Fig. 7. The data acquisition is only done at the start of the combustion engine for a short duration. The method does not require the data to be processed instantly, an idle time of the ECU can be used to perform the evaluation of the data. The measured terminal voltage and current signal as well as the actual temperature can be stored without using much memory. This data acquisition is repeated on every start of the combustion engine after a longer resting period of the battery, resulting in measurements in a balanced state of the battery cell. Therefore,

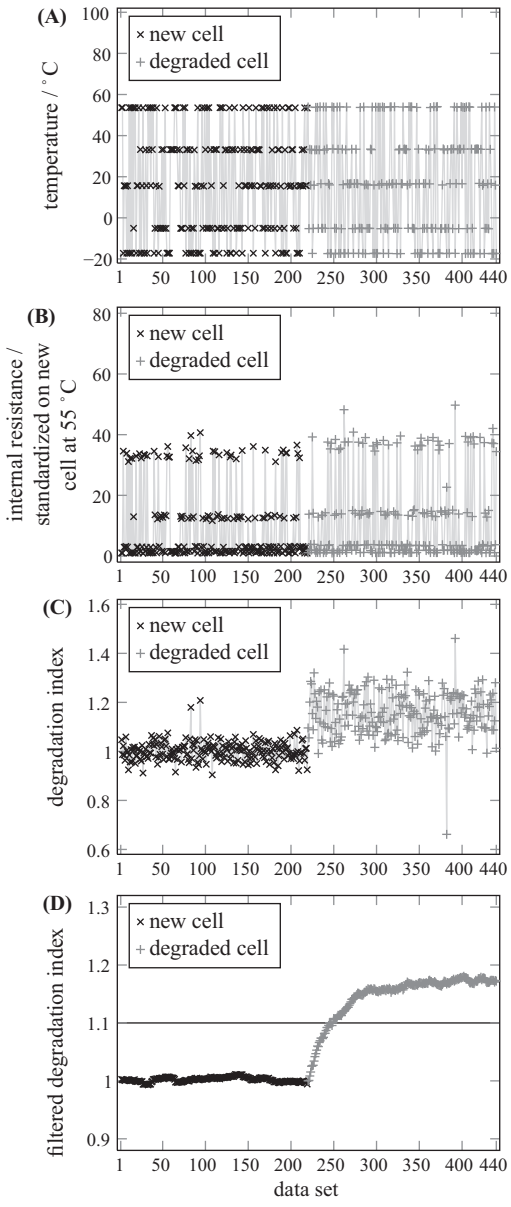


**Fig. 8.** (A–D) On-board application of the monitoring algorithm.

the measured temperature equals the real inner temperature of the battery. As the temperature has a great effect on the calculation of the degradation index from the internal resistance, which is identified using a low-effort recursive least-square estimator, this measurement must be as accurate as possible. The calculated degradation index is filtered, evaluated for an increase or a limit violation, and finally stored for further runs of the algorithm.

The application of the presented method on testing data from the laboratory is shown in Fig. 8. More than 200 data sets of the identification signal at the start of the combustion engine were recorded for a new and a degraded cell. The data sets of every single cell were randomly arranged. For the pairs of values consisting of temperature (plot A) and internal resistance (plot B), the degradation index (plot C) is calculated using (12). The degradation index for each of the two cells is almost constant with only few outliers caused by an inaccurate determination of the identification moment. As only two different states of degradation were available in measurement data, the degradation index changes abruptly when going from the new to the degraded cell. To remove the effect of the outliers and to give the degradation index a smooth appearance, a low-pass filter was applied to the values in plot C. The result is shown in plot D. The filtered degradation index now is flat, but shows a slower increase (from data set 220 to 350) due to the filter dynamics instead of the instantaneous change in the measurements. That means that abrupt changes can only be observed with some delay due to the filter dynamics. This is no constraint because the degradation in the vehicle is expected to show a slow progression, i.e. the prompt change from the new to the degraded cell is a worst-case scenario.

As the used filter can be a first-order low-pass filter, only the recent degradation index and not the whole history of data points or identification signals has to be stored. To recognize a possible failure, a limit defining the faultless operation region can be set up and compared with the calculated degradation index to advice the driver to have the battery system checked for possible failures. An example limit of 1.1, which is a serious degradation, is outlined in plot D of Fig. 8. Despite the worst-case scenario, the limit is exceeded by the filtered degradation index already after less than 25 data sets from the degraded cell.

If the impact of the operation mode is to be analyzed, the history of the degradation index should be stored. In connection with load and power profile, it can give a conclusion how different operation affects the degradation of the battery cells.

## 5. Conclusions

In this contribution, a method for the on-board determination of an internal resistance dependent degradation index in a hybrid vehicle was presented. The internal resistance is defined using an equivalent circuit and approximately incorporates the ohmic resistance and the polarization effect of a battery cell, which are not SOC dependent for the investigated cell type. The equivalent circuit was adapted to the identification signal, which is a terminal voltage and current measurement of low duration at the start of the combustion engine of the hybrid vehicle. Since this signal shows always a similar current profile, taking special care of the parameter dependence on current magnitude is not necessary in our algorithm. From the identified parameters, the internal resistance is calculated. Furthermore, a method to separate the different effects of temperature variation and degradation by intelligent data selection is presented. Using this method, a degradation index can be determined, which can be postprocessed to receive a smooth, robust index. All presented methods were developed with the main focus on the implementation of the algorithm in an on-board ECU. The algorithm proves low computational effort and results in a robust monitoring of the battery cell with the demonstrated degradation index.

As the influence of the temperature of the battery cell is as high as demonstrated, further research will be done on exact determination of the inner cell temperature also in dynamic load scenarios, when the sensor signals are not reliable anymore due to temperature gradients in the cells.

## References

[1] F. Huet, J. Power Sources 70 (1998) 59–69.
[2] U. Tröltzsch, O. Kanoun, H.-R. Tränkler, Tech. Messen 71 (2004) 509–518.
[3] S. Buller, Impedance-Based Simulation Models for Energy Storage Devices in Advanced Automotive Power Systems, Shaker, Aachen, 2003.
[4] U. Tröltzsch, Modellbasierte Zustandsdiagnose von Gerätebatterien, VDI Verlag, Düsseldorf, 2006.
[5] G.L. Plett, J. Power Sources 161 (2006) 1356–1368.
[6] G.L. Plett, J. Power Sources 161 (2006) 1369–1384.
[7] D. Andre, M. Meiler, K. Steiner, C. Wimmer, T. Soczka-Guth, D.U. Sauer, in: Proceedings of 12th Ulm ElectroChemical Talks, J. Power Sources, 2010, p. 57.
[8] D. Andre, M. Meiler, K. Steiner, H. Walz, T. Soczka-Guth, D. Sauer, J. Power Sources 196 (2011) 5356–5363.

[9] E.V. Thomas, H.L. Case, D.H. Doughty, R.G. Jungst, G. Nagasubramanian, E.P. Roth, J. Power Sources 124 (1) (2003) 254–260.
[10] F. Zhang, G. Liu, L. Fang, in: IEEE International Conference on Robotics and Automation, 2009, pp. 1863–1868.
[11] C. Barlak, Y. Ozkazan, in: International Conference on Electrical and Electronics Engineering, 2009, pp. II-101–II-105.
[12] E. Hairer, G. Wanner, Solving Ordinary Differential Equations: Stiff and Differential-Algebraic Problems, 2nd ed., Springer, Berlin, 2002.
[13] L. Ljung, System Identification: Theory for the User, 2nd ed., Prentice Hall, Upper Saddle River, 1999.
[14] B.Y. Liaw, E.P. Roth, R.G. Jungst, G. Nagasubramanian, H.L. Case, D.H. Doughty, J. Power Sources 119–121 (2003) 874–886.